ANNUAL REVIEWS

*Annual Review of Biophysics*

# Ball-and-Chain Inactivation in Potassium Channels

Nattakan Sukomon,[1] Chen Fan,[1,*] and Crina M. Nimigean[1,2]

[1]Department of Anesthesiology, Weill Cornell Medical College, New York, New York, USA; email: crn2002@med.cornell.edu

[2]Department of Physiology and Biophysics, Weill Cornell Medical College, New York, New York, USA



Annu. Rev. Biophys. 2023. 52:91–111

First published as a Review in Advance on January 10, 2023

The *Annual Review of Biophysics* is online at biophys.annualreviews.org

https://doi.org/10.1146/annurev-biophys-100322-072921



*Current address: Science for Life Laboratory, Department of Biochemistry and Biophysics, Stockholm University, Solna, Sweden



## Keywords

ball-and-chain inactivation, voltage-gated $K^+$ channel, $Ca^{2+}$-activated $K^+$ channel, $Na^+$ channel, N-type inactivation

## Abstract

Carefully orchestrated opening and closing of ion channels control the diffusion of ions across cell membranes, generating the electrical signals required for fast transmission of information throughout the nervous system. Inactivation is a parsimonious means for channels to restrict ion conduction without the need to remove the activating stimulus. Voltage-gated channel inactivation plays crucial physiological roles, such as controlling action potential duration and firing frequency in neurons. The ball-and-chain moniker applies to a type of inactivation proposed first for sodium channels and later shown to be a universal mechanism. Still, structural evidence for this mechanism remained elusive until recently. We review the ball-and-chain inactivation research starting from its introduction as a crucial component of sodium conductance during electrical signaling in the classical Hodgkin and Huxley studies, through the discovery of its simple intuitive mechanism in potassium channels during the molecular cloning era, to the eventual elucidation of a potassium channel structure in a ball-and-chain inactivated state.

## Contents



## 1. INACTIVATION IN THE EARLY DAYS OF ION CHANNEL RESEARCH

Ion channels that select for sodium and potassium ions, called $Na^+$ and $K^+$ channels, are crucial for the electrical activity of the brain. Strict orchestration of channel activation as well as closure is needed for the generation of an action potential (**Figure 1**). These channels are activated by changes in membrane voltage, and the ensuing ion fluxes across the membrane through open channels further modify the voltage across the membrane. Termination of ion flux can happen in two ways: (*a*) regular channel closure due to removal of the stimulus and (*b*) inactivation, which is a different type of channel closure that occurs while the stimuli are still present (53). In $Na^+$ channels, inactivation is crucial for shaping the action potentials and setting the resting voltage for the next round of firing (143), while in $K^+$ channels, it regulates action potential duration and firing frequency of nerve and muscle (40, 53). Inactivation can occur on various timescales (milliseconds to seconds) and plays important roles in many ion channels, not only in the action potential, but also in many other physiological processes.

Fast inactivation for voltage-gated $Na^+$ (NaV) channels involved in the action potential of squid giant axons was first proposed in the 1950s in the classic studies on squid giant axons by Hodgkin & Huxley (55). In the study, Hodgkin & Huxley reported inactivation of the $Na^+$ permeability in which the $Na^+$ current increased upon depolarization of the voltage-clamped fiber and then spontaneously decreased even though the membrane potential remained constant.

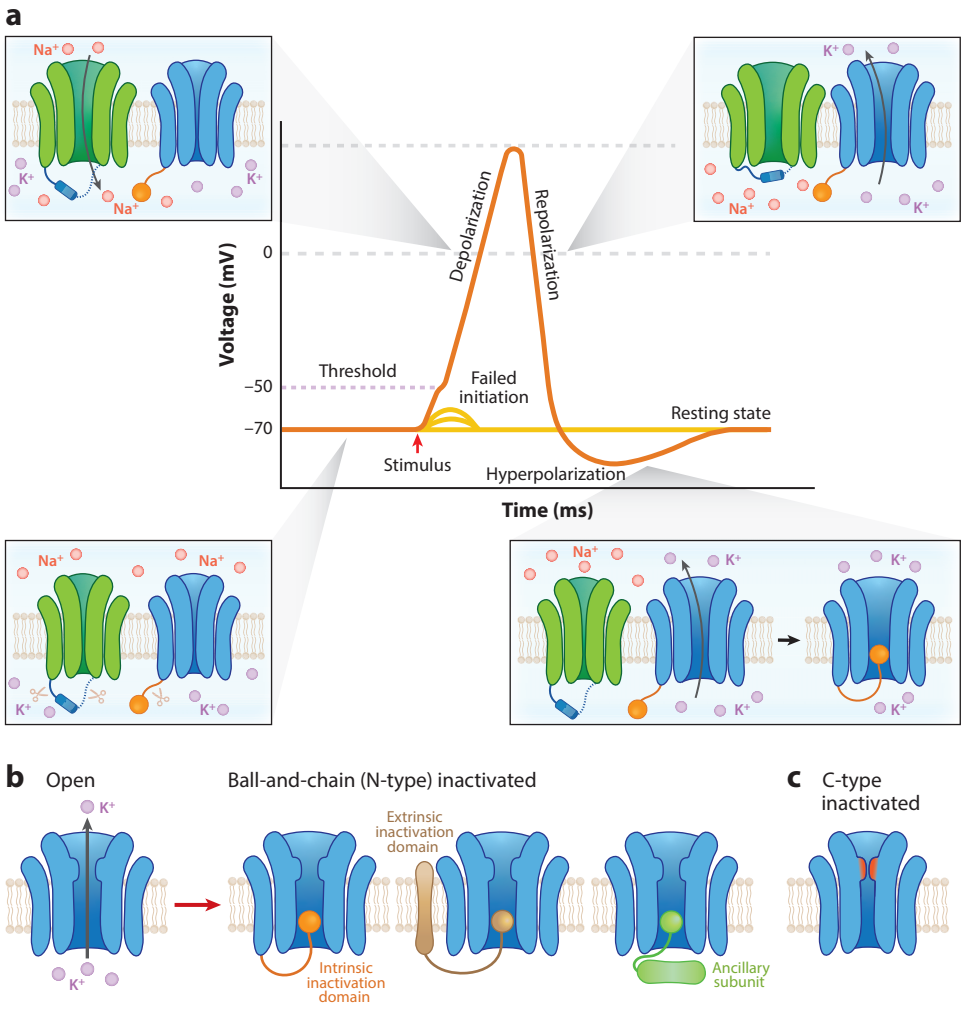


**Figure 1**

Ion channel gating contributing to action potentials. (*a*) Interplays between NaV (*green*) and Kv (*blue*) channels during action potentials. The inactivation of NaV is mediated by the highly conserved IFM motif on the III–IV linker (*blue bar*). The inactivation of Kv happens via pore occlusion by the N-terminal ball motif (*orange sphere*). The selectivity filters were omitted for simplicity. The IFM motif and the N termini are cleavable by proteolytic agents (denoted as scissors), leading to the elimination of fast inactivation, as shown in the early studies. (*b*) Different sources for N-terminal inactivation domains. The ball-and-chain inactivation is mediated by an intrinsic inactivation domain (*orange*), or by an extrinsic inactivation domain from a transmembrane auxiliary subunit (*brown*) or a cytoplasmic ancillary subunit (*green*). (*c*) C-type inactivation. Various $K^+$ channels can undergo C-type inactivation, which is mediated by conformational changes at the selectivity filter (*orange highlight*). Abbreviations: IFM, isoleucine, phenylalanine, methionine; Kv, voltage-gated $K^+$; NaV, voltage-gated $Na^+$.

They proposed that three charged particles, which they denoted "m," were responsible for the $Na^+$ channel activation, and one more highly charged particle, denoted "h," brought about the channel inactivation (1, 6, 55). In 1973, Armstrong and colleagues (9, 13) showed that the fast inactivation of $Na^+$ channels could be irreversibly eliminated by perfusing proteolytic enzymes in squid axons, suggesting a flexible inactivation domain, while the activation gates remained

unaffected (**Figure 1**). The $K^+$ conductance was also found early on to exhibit inactivation (9, 85), and inactivation of both $Na^+$ and $K^+$ channels could be mimicked by a variety of pharmacological agents, such as TEA derivatives, local anesthetics, pancuronium, and *N*-propylguanidinium, as well as antibodies when applied intracellularly but not extracellularly, suggesting that the inactivation gate was cytosolic (10, 13, 27, 73, 126, 142).

The Hodgkin & Huxley (55) study proposed that gating particles carrying charges through the electric field generated by a transmembrane voltage are associated with both activation and inactivation of the $Na^+$ conductance, thus assigning voltage dependence to both processes (55). Such movement of charged gating particles was predicted to generate current and was indeed later measured as gating current. In 1977, Armstrong & Bezanilla (12) found that inactivation had little intrinsic voltage dependence, as there was no charge movement directly associated with it; instead, it garners its voltage dependence indirectly by simply being coupled to the voltage-dependent activation. A similar trend was later documented for $Na^+$ channels in other organisms (3, 87).

Due to the discoveries that inactivation can be removed by proteolytic agents, can be mimicked by various pharmacological agents perfused internally, and is not voltage dependent, Armstrong & Bezanilla (12) proposed a ball-and-chain model to explain fast inactivation. In this model, an inactivation particle (ball) is tethered to a cytosolic, unstructured, protease-cleavable segment of the ion channel (chain) (**Figure 1**). Channel inactivation occurs when the inactivation ball binds to its receptor at the inner mouth of the channel and occludes the channel pore. The receptor for the inactivation ball is thus only available once the channel is activated, illustrating the coupling between activation and inactivation (1, 2, 6, 12, 69). It was not until 43 years later that structural evidence for this intuitively described mechanism became available and the original name was structurally validated (38, 149).

## 2. INACTIVATION IN THE MOLECULAR CLONING ERA

With the development of molecular cloning and the cloning of $Na^+$ and $K^+$ channels in the mid-1980s, the inactivation mechanism had been thoroughly investigated, starting with voltage-gated $K^+$ (Kv) channels (14, 44, 50, 70, 99, 110, 121, 124, 130, 133). $K^+$ channels exhibit fast inactivation similar to that of $Na^+$ channels, although this was not previously documented by the classic studies of Hodgkin & Huxley (see 8–10, 30). Shaker was the first $K^+$ channel to be cloned, from the muscle of *Drosophila melanogaster*, a voltage-gated channel that mediates a transient A-type $K^+$ current caused by the rapid inactivation of the channel upon opening with depolarization (15, 92, 116, 120). Variants of Shaker $K^+$ channels with differences in cytoplasmic domains due to alternative splicing show different inactivation rates (4, 84, 121, 122, 145). Kv channels have been shown to share the same architecture (see **Figure 3** below), with six transmembrane-spanning helices, of which the first four are proposed to constitute a voltage sensor domain and the last two the pore domain, which contains a highly conserved signature sequence, part of the selectivity filter defining the high selectivity of these channels for $K^+$ (47, 48, 61).

### 2.1. Ball-and-Chain (N-Type) Inactivation

Similar to what had previously been observed for $Na^+$ channels, inactivation of Shaker $K^+$ channels could be eliminated when trypsin was applied intracellularly to Shaker channel–expressing *Xenopus laevis* oocytes (56), confirming that the inactivation apparatus was located on the cytosolic channel side (47, 48, 61). The inactivation process in Shaker was found to resemble currents modified by open pore blockers such as quaternary ammonium agents (8, 35). These lines of evidence further supported the existence of a ball-and-chain inactivation mechanism similar to that proposed previously for $Na^+$ channels.

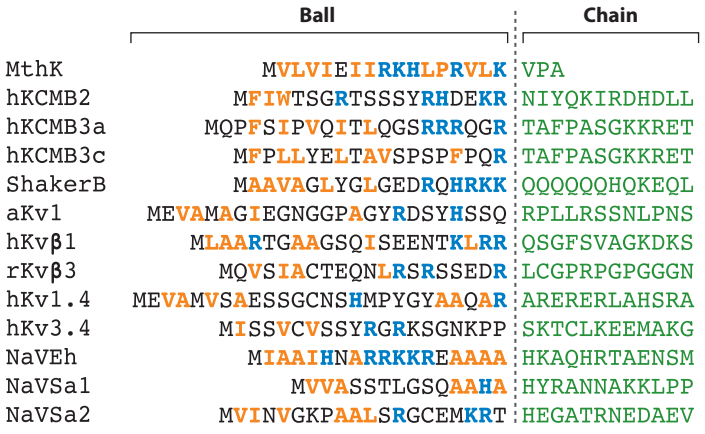


**Figure 2**

Sequence alignment showing N-terminal ball and chain domains from MthK (accession number CEP 36137), human KCMB2 (BK β2, accession number NP_001265840.1), human KCMB3a (BK β3a, accession number NP_741979.1), human KCMB3c (BK β3c, accession number NP_741981.1), *Drosophila* Shaker B (accession number CAA 29917), Aplysia Kv1 (accession number NP_001191634.1), human Kvβ1 (accession number Q14722.1), rat Kvβ3 (accession number Q63494.1), human Kv1.4 (accession number NP_002224.1), human Kv3.4 (accession number NP_001034663.1), *Emiliania huxleyi* NaVEh (accession number CAMPEP_0187654740), *Scyphosphaera apsteinii* NaVSa1 (accession number CAMPEP_0119314838), and *Scyphosphaera apsteinii* NaVSa2 (accession number CAMPEP_0119345692). Orange letters and blue letters represent hydrophobic and positively charged residues in the ball motifs, respectively. Green letters represent residues in the chain regions.

The ready availability of the Shaker $K^+$ channel clone rapidly advanced the field. Genetic manipulations of the N terminus of Shaker (approximately 83 residues) such as deletion of the first approximately 20 residues eliminated fast inactivation (56). A synthetic peptide with a sequence corresponding to the first 20 amino acids of Shaker when applied to the cytoplasmic side of the channel restored inactivation of the noninactivating Shaker B (ShB) channel (ShB Δ6–46), with kinetics similar to the inactivation of the full-length channel (146). Based on these observations, the inactivation domain (or inactivation gate) of Shaker was located at the N terminus of the channel. The first 20 N-terminal residues were proposed to function as a ball that enters the pore at the cytoplasmic face of the channel and occludes the ion passage. The remainder of the N terminus presumably acted as the chain that tethered the ball (56) (**Figure 2**). The ball motif could be further separated into a hydrophobic region at the N-terminal half followed by a hydrophilic region. The general requirement for effective inactivation was for the majority of residues at the N-terminal part of the ball to be hydrophobic, and most of the residues at the C-terminal end to be positively charged (2, 4, 56, 84, 146) (**Figure 2**). Further studies on the stoichiometry of inactivation revealed that only one N-terminal ball from a $K^+$ channel tetramer was required (76).

## 2.2. C-Type Inactivation

Since the inactivation domain was originally found at the N terminus of the Shaker $K^+$ channel, the ball-and-chain mechanism also became referred to as N-type inactivation. The distinction arose because a slower, residual inactivation was observed upon N-terminus deletion and was dubbed C-type inactivation because it varied between the two C-terminal splice variants of Shaker (75). C-type inactivation refers to an inactivation mechanism in which ion flow through channels is

regulated by conformational changes of the selectivity filter (32, 77, 94, 115, 125, 138), which locates near the extracellular side of the pore (**Figure 1*c***). The precise nature of the conformational change of the selectivity filter associated with C-type inactivation is somewhat controversial, but the consensus is that this change is modulated by filter ion occupancy and concentration of permeant ions on the extracellular side (17, 21, 31–33, 69, 75, 77, 94, 115, 125, 138, 151).

Both N- and C-type inactivation mechanisms are important for shaping the action potential: The ball-and-chain inactivation regulates the duration of the action potential by blocking $K^+$ efflux during repolarization, while C-type inactivation controls the number of conducting channels and is a rate-limiting step for recovery (80). Ball-and-chain inactivation and C-type inactivation can coexist and be either independent or allosterically coupled, depending on the channel (57, 102, 139). Coupling of the ball-and-chain and C-type mechanisms has been studied in Shaker and mammalian Kv channels (16, 20). The binding of the N-terminal ball is shown to increase the rate of C-type inactivation (16). It is hypothesized that the coupling occurs via at least two mechanisms, the clearance of $K^+$ from the selectivity filter after pore occlusion by the N-terminal ball and large-scale changes in general protein conformation (16, 20). C-type inactivation is also found in prokaryotic NaV channels (65, 103).

## 3. MOLECULAR DETERMINANTS FOR BALL-AND-CHAIN INACTIVATION IN $K^+$ CHANNELS

It was later discovered that ball-and-chain inactivation in $K^+$ channels was not restricted to N-terminal domains that are intrinsic to the channel. N-terminal domains of specific accessory subunits that modulate $K^+$ channels, such as β subunits of Kv channels (14, 50, 99, 133), as well as large-conductance $Ca^{2+}$-activated $K^+$ channels (44, 70, 124, 130), can also play the role of causing N-type inactivation (104, 129) using N-terminal ball peptides conserved in length and hydrophobicity character (**Figures 1*b*** and **2**). Some of these subunits are discussed in the following sections.

### 3.1. Properties of the Ball Motif

Synthetic peptides were among the early tools used for investigating the characteristics of the ball domain required to elicit an effective inactivation. Murrell-Lagnado & Aldrich (84) demonstrated that synthetic peptides resembling the N-terminal balls from different Shaker variants were able to block noninactivating ShB (Δ6–46) with a rate similar to that occurring in the intact Shaker channels, even though the peptides shared no strict sequence similarity. In addition, ball peptides from one $K^+$ channel can inactivate other $K^+$ channels (39, 60, 66, 80, 84, 123). The original ShB ball peptide also induced a ball-and-chain inactivation–like block in the prokaryotic $K^+$ channel KcsA, which only undergoes C-type inactivation (80). These results suggested that ball-and-chain inactivation had low specificity requirements, although a rather loose dual hydrophobic and electrostatic ball characteristic appeared to be needed (**Figure 2**).

N-terminal ShB-like peptides containing only charged residues were not effective in inactivating the channel (146). Mutation of a leucine (Leu7 in ShB) to glutamate significantly reduced the binding affinity of the peptide to the channel (56, 146), while substituting Leu7 for other hydrophobic residues produced only small changes (84). Hydrophobicity of the first half of the ball peptide was necessary for stabilizing the ball in its channel-bound, inactivated state; the remaining hydrophilic region was involved in long-range electrostatic interactions, rather than specific interactions between peptide and channel (84, 146). The overall charge of the hydrophilic region affected the inactivation on-rate, presumably by increasing the effective concentration of the

peptide near the binding site ($k_{on}$). While increasing the net positive charge accelerated inactivation, decreasing the net positive charge or reversing the net charge to negative decelerated the inactivation (4). Thus, while the specificity for binding to the channel is low, ball peptides should be hydrophobic for the N-terminal half and have a net positive charge for the second half for effective inactivation to occur (**Figure 2**). Inactivation-inducing ball peptides of β subunits of Kv (14, 50, 99, 133) and large-conductance $Ca^{2+}$-activated $K^+$ (BK) (44, 70, 124, 130) channels display similar characteristics.

### 3.2. Properties of the Chain

The roles played by the chain region in inactivation kinetics are still inconclusive. Hoshi et al. (56) tested a series of mutations in the chain region (residue 20–83) of the ShB channel. Shortening the chain region by deletion tends to speed up the inactivation, and lengthening the chain region by insertion tends to slow down the inactivation. However, not all deletion and insertion mutations follow this trend. The chain regions of other Kv channels contain charged residues whose substitution with Ala slow down inactivation, although to a lesser extent compared to similar substitutions in the hydrophobic region of the ball motif (101). These studies suggest that the chain motif might be involved in shaping inactivation kinetics of Kv channels. However, studies are still needed to decipher the exact roles of the chain region.

In contrast, a thorough study of inactivation produced by the β2 subunit of BK channels (137) reached the conclusion that almost any amino acid sequence can serve as an adequate chain, as long as it contains a minimum of 12 residues between the transmembrane part and a hydrophobic residue triplet located at the very N terminus, which appears to be critical for inactivation.

### 3.3. Early Structures of the Ball Peptide

Early structural studies of the inactivation domain of $K^+$ channels were conducted using high-resolution nuclear magnetic resonance (NMR) spectroscopy on isolated unbound peptides. NMR analysis of inactivation peptides with almost no homology in primary sequences (from mammalian Kv3.4 and Kv1.4 channels) shows that these peptides are well-defined in aqueous solution but have distinct structures (7). In contrast, inactivation peptides of other $K^+$ channels appear to be unstructured in solution. The first 22 amino acids of ShB (Sh-P22, also known as Shaker inactivation ball domain) do not have a compact structure in solution (109). The NMR analysis of the first 45 amino acids of the auxiliary β2 subunit (KCNMB2) of the BK channel containing both a ball motif (residue 1–17) and a chain motif (residue 20–45) suggests that there is a flexible N terminus anchored to a helical chain domain (19). Studies using synthetic peptide and mutagenesis have suggested that ball peptides adopt some conformations that expose their hydrophobic residues when bound to the pore (84).

## 4. BALL-AND-CHAIN INACTIVATION MODELS

### 4.1. Structure–Function Studies of Ball-and-Chain Inactivation in Kv Channels

A structure–function investigation of ball-and-chain inactivation provided by an ancillary β subunit of a mammalian Kv channel (Kv1.4) led to a model where the ball domain of the inactivation peptide binds deep into the pore (rather than just occluding the pore mouth) in a fully extended conformation (150). The study included systematic mutagenesis of both the pore domain of the Kv channel and the ball peptide of the β subunit, as well as a structural analysis of the KcsA channel bound with a blocker [TBSb, an analog of tetrabutyl ammonium (TBA), a known open pore blocker of Kv channels (35, 150)] that mimicked the inactivation phenotype. The finding that the same pore residues were able to functionally interact with the ball peptide and to structurally

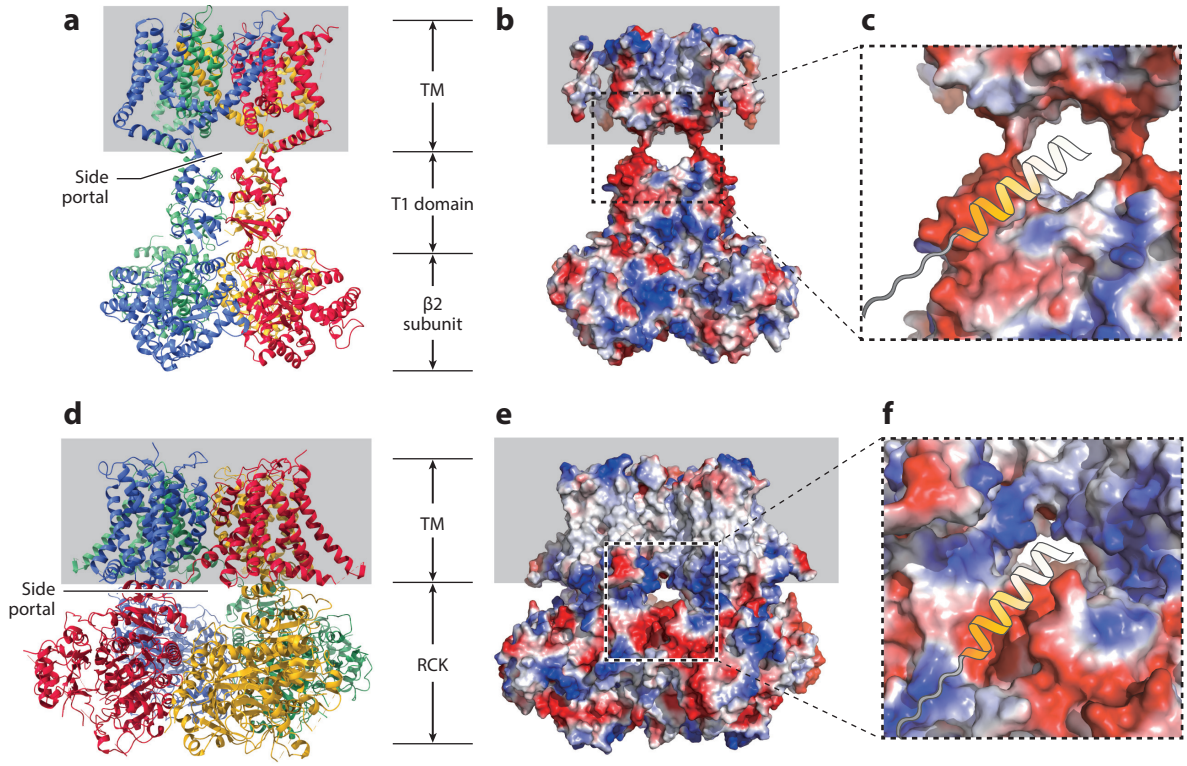


**Figure 3**

Side portals as a hypothetical entryway for the N-terminal ball motifs to channel pores. (*a*) Structure of rat Kv1.2-Kvβ2 complex (PDB ID 2A79) with each subunit in different colors (*b*) Surface potential representation of the Kv1.2-Kvβ2 complex. (*c*) Zoomed-in view of the side portal. Yellow and white ribbons represent the hydrophilic and hydrophobic regions of a putative ball, respectively, with the chain shown as a string, reaching the pore via the side portals. (*d*) Structure of human BK channel bound with $Ca^{2+}$ (PDB ID 6V38). Each subunit is colored differently. (*e*) Surface potential representation of the BK channel (PDB ID 6V38). (*f*) Zoomed-in view of the side portal. The ball and chain are shown in similar representation as in panel *c*. The positively charged residues in the C-terminal end of the ball (*dark yellow* in panels *c* and *f*) presumably electrostatically interact with the negatively charged residues in the lateral window of the channel (*red*), leading the ball motif to the pore. Abbreviations: BK, large-conductance $Ca^{2+}$-activated $K^+$; PDB, Protein Data Bank.

interact with the blocker bound in the pore led to one of the most detailed prestructure models of ball-and-chain inactivation in Kv channels.

At the same time, the hydrophilic region of the inactivation peptide was proposed to bind outside the pore at the side portals, the aqueous protein surfaces above the cytoplasmic domains of the channel (T1 domains) (45, 67, 112) (**Figure 3**). A crystallographic study of a Kv channel (Kv1.2) in complex with a β subunit (β2) proposed that the same portals function as access routes for β subunit ball entry into the pore (74). The N-terminal part of Kv1.2 forms the cytoplasmic T1 domain, and the β2 subunit binds below the tetrameric assembly of the T1 domain. The side portal between the membrane and the T1 domain connects directly to the open pore, and a surface potential analysis showed a negatively charged ridge below the portal (**Figure 3**). Although the β2 subunit lacks the inactivating N terminus, its homology to the inactivating β1 subunit allows one to deduce a probable path of entry into the pore for the ball via the side portals. The negatively charged ridge would help attract the positively charged ball, and the resolved residues in the β2 N terminus have the length range of the chain.

## 4.2. Structure–Function Studies of Ball-and-Chain Inactivation in Large-Conductance $Ca^{2+}$-Activated $K^+$ Channels

Similar portals were proposed to be the access routes for the inactivation ball in BK channels, where inactivation can occur only via coassembly with accessory subunits (43). BK channels have a similar architecture to Kv channels in the membrane portion, with a $K^+$-selective pore and voltage sensor domains (**Figure 3*d***). In addition, they also have a large cytosolic domain that binds $Ca^{2+}$, which contributes to pore opening (140). The β subunits of BK channels are different than the soluble β subunits of Kv channels (**Figure 1**) in that they have two membrane-spanning helices connected by a large extracellular loop, with their N and C termini in the cytoplasm (129). Only the β2, β3a, and β3c inactivating subunits have, in addition, a section of extra residues at the N terminus, similar to the inactivating sequences in the Kv channels and the β subunits of Kv channels (**Figure 2**). The synthetic peptide of the β3a ball is sufficient to inactivate the BK channels, and the binding of the peptide competes with the binding of the open pore blocker TBA, indicating that the blocking sites for both the blocker and the inactivation ball are located in the BK channel cavity (44).

A structure of the BK channel in complex with the β4 subunit reveals its mode of binding within the complex (118). Although the β4 subunit does not have the inactivating N terminus, its pose allows one to infer that a ball attached to an equivalent inactivating β subunit gets to its binding site in the pore via the side portals. Similar to the side portal in Kv1.2, the portal of the BK channel has a negative charged groove potentially attractive to the positive charged cluster of the ball (**Figure 3*e–f***).

Nevertheless, despite numerous attempts, no structures of Kv or BK channels in a ball-and-chain-like inactivated conformation have been captured to date.

## 4.3. First Structural View of Ball-and-Chain Inactivation in a $K^+$ Channel

Almost 70 years after inactivation was proposed to quantitatively model the action potential (55), the development of single-particle high-resolution cryo-electron microscopy (cryo-EM) technology allowed the successful capture of ball-and-chain inactivation in structures of an archaeal $Ca^{2+}$-activated $K^+$ channel, MthK (38) (**Figure 4**), the first pictorial evidence of the mechanism. MthK is from *Methanobacterium thermoautotrophicum* and is a member of the BK channel family. MthK channels are $K^+$ selective, are activated by cytosolic $Ca^{2+}$, and contain RCK-like $Ca^{2+}$-sensing domains, similar to BK channels. Unlike BK channels, they only contain the two transmembrane domains that define the conserved $K^+$ pore and lack voltage-sensing domains (63, 71, 95, 144). Since MthK has only the $Ca^{2+}$-gating machinery and expresses well in *Escherichia coli*, it had been a heavily utilized and faithful model for $Ca^{2+}$ gating in BK channels. Indeed, to date, many structures of MthK channels in different conformations have been accurately assigned to functional states (36, 38, 63, 141) (**Figure 4**), while the correspondence between BK channel structures and states is less well understood (117, 118).

MthK channels had been shown to undergo inactivation when assayed in spheroplasts and liposomes, and truncation of the 17 N-terminal residues fully abolished inactivation (38, 68, 100). In 2020, Fan and colleagues (38) determined the cryo-EM structures of MthK in both the presence and absence of $Ca^{2+}$, which revealed not only the bundle-crossing gate of the channel in two clearly distinct conformations (corresponding to open and closed channels, respectively) but also the very N terminus of only one of the four subunits of the MthK tetramer, inserted into the open channel pore (**Figure 4**). The inactivation ball motif of MthK consists of the first approximately 17 N-terminal amino acids that are entirely contained within and plug the pore, tethered to the first helix (TM1) of the first transmembrane domain of the channel via a three-amino-acid-long

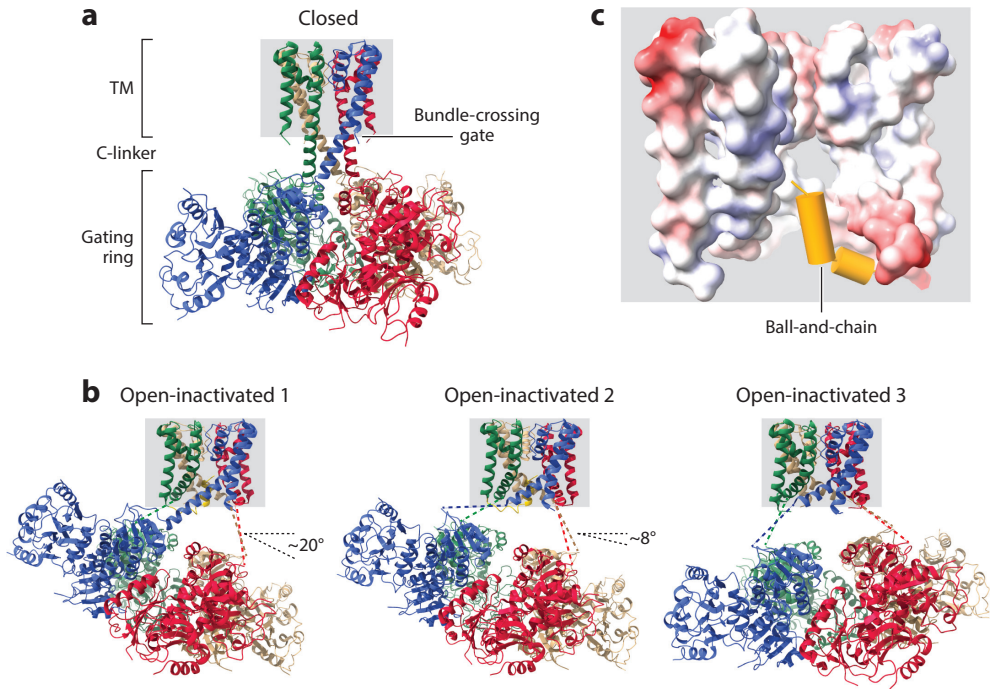


**Figure 4**

Structures of MthK (*a*) in closed state ($Ca^{2+}$ free; PDB ID 6U6D) and (*b*) in three different open-inactivated states ($Ca^{2+}$ bound), with highly tilted (PDB ID 6U68), moderately tilted (PDB ID 6U6E), and mildly tilted (PDB ID 6U6H) RCK domains. Each subunit is colored differently. The ball-and-chain inactivating domain is colored gold. (*c*) Surface potential representation of the MthK transmembrane region (created using PDB ID 6U68). The ball-and-chain inactivation motif is shown in gold. One subunit is omitted for clarity. Abbreviation: PDB, Protein Data Bank.

chain (38, 68) (**Figure 2**). In the cryo-EM structure, the peptide containing the first 13 residues forms a helical structure that inserts vertically along the central axis of the channel pore up to the selectivity filter and occupies most of the space in the large pore cavity. The rest of the N-terminal motif (residue 14–20) forms a loop connecting it with the TM1 helix (38) (**Figure 4*c***).

The first 17 N-terminal residues form the inactivation ball, which shares the characteristics of all other ball sequences; the first half is hydrophobic and forms the tip that burrows deep into the pore, interacting with the hydrophobic channel cavity (**Figure 2**). The latter half, the base, is heavily positively charged and engages in long-range electrostatic interactions with the intracellular part of the channel pore mouth, which is overall negatively charged, to guide the ball into the pore. Just like in Kv and BK channels (see above), mutation of the first few hydrophobic residues dramatically affects inactivation (68). The chain (three amino acids) is shorter than the documented chains of other $K^+$ channels (**Figure 2**), although this may be explained by the shorter distance needed for the ball to travel to plug the pore, since MthK does not have voltage sensor domains to stand between the N-terminal ball and the pore.

In addition, the position of the MthK $Ca^{2+}$-gating ring in the open state is not fixed, as seen in the crystal structure (63); instead, it tilts and rocks with respect to the transmembrane domains, creating large spaces through which a ball domain can conceivably sneak into the pore (**Figure 4**). The gating ring's flexibility comes from it being suspended under the pore domain via four flexible tethers, the C-linkers that connect each pore-forming helix to the RCK ring (**Figure 4*b***). The

C-linkers, presumably unfolded into disordered loops upon channel opening and thus no longer visible in the structures, allow the gating ring to adopt different tilt angles with respect to the transmembrane domain. The packing of full-length MthK into 3D crystals (63) likely prevented the different conformations of the gating ring observed in the cryo-EM study and the development of an open state conducive to entry of the ball domain into the pore, which may explain why the ball-and-chain inactivated MthK was not observed in previous crystallography studies.

## 4.4 Alternative Binding Sites for the Ball Motif When Outside the Pore

The binding site of one ball peptide in the pore has been identified (for MthK channels); however, it is still not understood what the other three ball domains do. Are they still folded, or are they disordered and floppy? Do they bind to any other domain of the channel, or do they bind to the membrane? The ball domains are also not resolved in the $Ca^{2+}$-free, closed MthK channel structure. An NMR study using an isolated $Ca^{2+}$-binding domain of MthK (RCK domain) and synthetic N-terminal peptides containing either the first 11 or the first 17 amino acids suggested that there is a direct interaction between the RCK domain and the peptides (68). Shorter peptides or long peptides containing a mutation that impairs inactivation abolished the interaction, suggesting some specificity and the possibility for regulation of the inactivation process (68). However, there is no high-resolution structural evidence for such potential interactions.

## 4.5. State Models for Ball-and-Chain Inactivation in $K^+$ Channels

A few models describing the kinetics of the ball-and-chain inactivation have been proposed. The single-step model of ball-and-chain inactivation is based on the early studies in the Shaker channel (35, 56, 84, 146) (**Figure 5*a***). In this model, the affinity of the N-terminal inactivation gate to the channel is largely dependent on the hydrophobicity of the ball motif and determines the fraction of blocked current. The single-step model assumes that the binding and blocking happen simultaneously. The inactivation is intrinsically voltage independent (but access to the pore requires voltage-dependent activation of the channel) (35).

The pre-inactivated (two-step) model has been proposed based on the investigations of Zhou et al. (150); in this model, the inactivation peptide first interacts with residues near the pore before entering and binding to the channel pore. The rate-limiting step in the model is binding to the first, pre-inactivated state (150) (**Figure 5*b***). The model assumes that binding to the pre-inactivated state occurs outside of the membrane electric field, making the inactivation nearly voltage independent. The two-step inactivation model was also proposed for ball-and-chain inactivation in BK channels (72). Other models in which the inactivation ball binds to several different sites on the channel before reaching the final site in the pore have also been proposed (97, 101) (**Figure 5*c***).

## 4.6. Lipid Regulation of Ball-and-Chain Inactivation

Given that ion channels are membrane proteins, the impacts of phospholipid membranes on inactivation are particularly important. A few studies suggested a role of phosphatidylinositol 4,5-bisphosphate (PIP2) in regulating the ball-and-chain mechanism. PIP2 is a lipid component of the inner leaflet of the membrane and plays an important role in signal transduction (88). It was proposed that the negatively charged headgroup of PIP2 can immobilize the positively charged residues of the N-terminal ball, given that intracellular application of PIP2 eliminates ball-and-chain inactivation of some Kv channels (88). Lipid microdomains, compartments of the membrane that are enriched with cholesterol and sphingolipids, are another possible regulator (34). They were shown to impact colocalized ion channels by direct lipid binding or by influencing

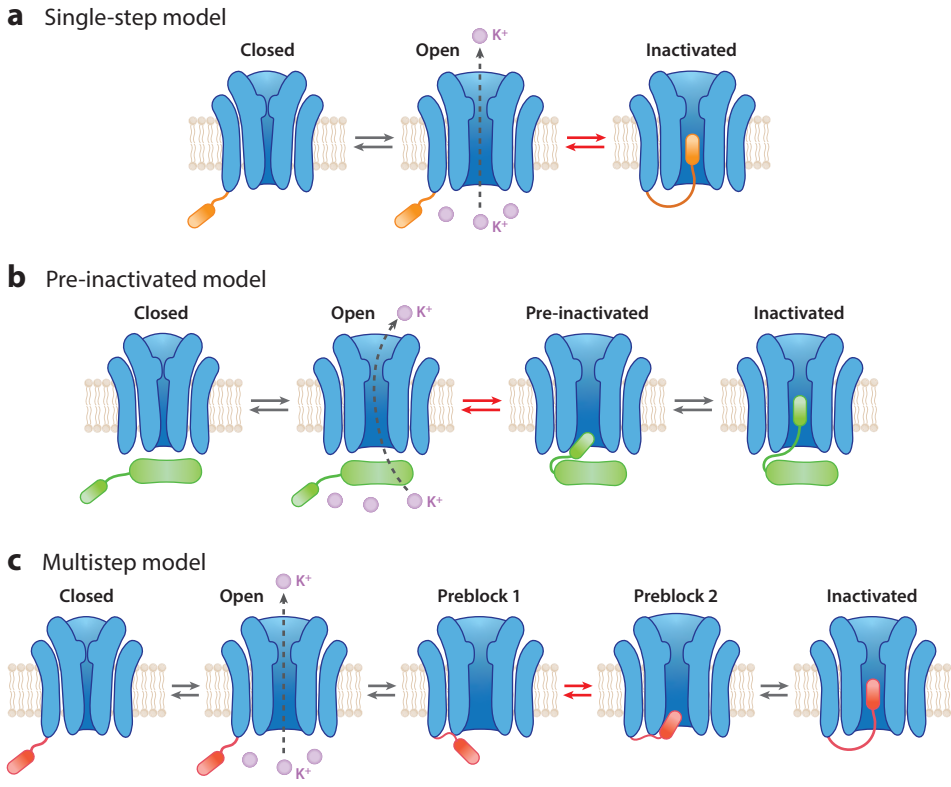


**Figure 5**

Models for ball-and-chain inactivation in $K^+$ channels. (*a*) Single-step model representing the coupling of channel opening and inactivation. The red arrows indicate the binding of the ball-and-chain motif to the channel pore, which happens simultaneously with pore occlusion. (*b*) Pre-inactivated model based on the study of Zhou et al. (150) with a chimeric Kv channel. The rate-limiting step (*red arrows*) is the formation of the pre-inactivated state from interactions of the ball motif with regions near the pore prior to pore occlusion. (*c*) Multistep model based on the study of Prince-Carter & Pfaffinger (101) using Aplysia Kv1. The rate-limiting step (*red arrows*) is the transition between a state where the inactivation peptide is bound to a region close to the pore (preblock 1) and a second state where the inactivation peptide is now bound at a different location, still not blocking the pore, but in a position to do so (preblock 2). Note that both preblock states are open and not blocked. Abbreviation: Kv, voltage-gated $K^+$.

the physical properties of the bilayers, such as thickness. In animal cells, various $K^+$ channels that can undergo ball-and-chain inactivation, such as Kv and BK channels, are located at the lipid microdomains (34). Activities of such channels can be modulated by cholesterol or bilayer thickness. However, the impact of lipid microdomains on ball-and-chain inactivation properties has yet to be elucidated.

## 5. COMPARISON TO THE INACTIVATION MECHANISM IN $Na^+$ CHANNELS

Even though NaV channels were the pillars of fast inactivation research (11–13, 55), their inactivation mechanism is still controversial. Paradoxically, even if the term ball-and-chain inactivation was originally coined to describe NaV channel inactivation, research on these channels almost

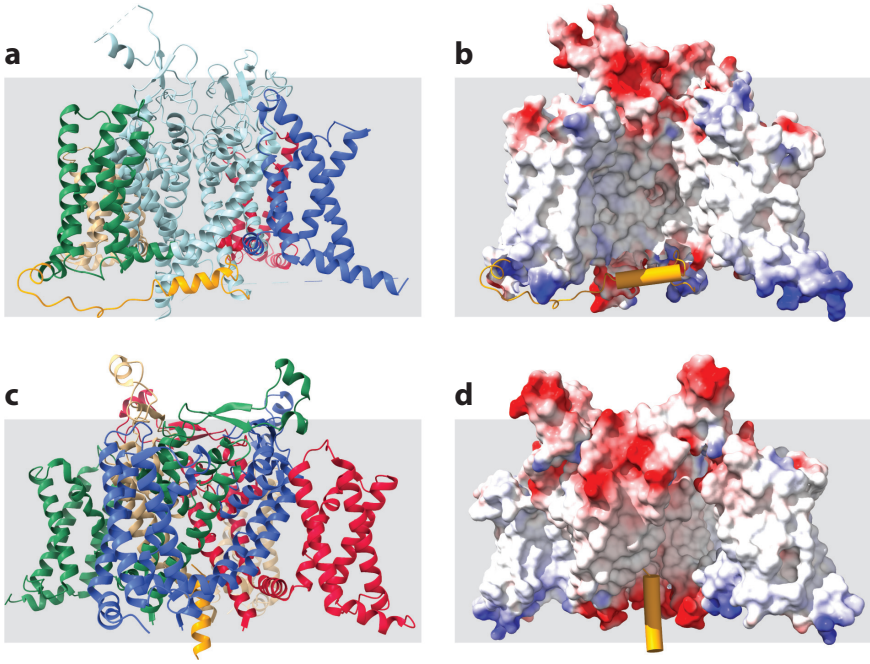


**Figure 6**

Structures of NaV channels. (*a*) Human NaV1.4 channel (*left*) (PDB ID 6AGF) with VSD I–IV, pore region, and IFM motif colored differently. (*b*) Surface potential representation of the channel and the IFM motif (*gold*) is shown with one subunit omitted for clarity. (*c*) *Emiliania huxleyi* NaVEh channel (*left*) (PDB ID 7X5V) with each subunit colored differently. The ball-and-chain inactivation motif is colored gold. (*d*) Surface potential representation of the channel (*right*) and the ball-and-chain motif (*gold*) with one subunit removed for clarity. Abbreviations: IFM, isoleucine, phenylalanine, methionine; NaV, voltage-gated $Na^+$; PDB, Protein Data Bank; VSD, voltage-sensing domain.

discarded this mechanism until very recently because most NaV channels studied to date appear to employ alternative ways to inactivate (42, 62, 65, 91, 93, 103, 113, 126, 127, 134).

In humans, nine types of NaV channels (NaV1.1–1.9) are present in nerve, muscle, heart, and other tissues (23). Unlike $K^+$ channels, eukaryotic NaV channels are organized as one single polypeptide chain divided into four homologous repeats (I, II, III, IV). Each repeat, similar in architecture to one $K^+$ channel subunit, has six transmembrane helices, including a voltage-sensing domain (first four helices) and a pore domain (last two helices) (22) (**Figure 6**).

Unlike $K^+$ channels, the inactivation motif of NaV channels is located in the cytoplasmic linker connecting repeats III and IV, with a signature sequence comprising three highly conserved amino acids, isoleucine, phenylalanine, methionine (IFM), at the beginning of the linker (113, 127, 134) (**Figure 6**). Antibodies bound to the III–IV linker region alter the inactivation rate when applied from the intracellular side (126), and deleting the linker eliminates inactivation (93). The IFM motif is the most critical, with mutation of I or M slowing and mutation of F fully abolishing inactivation of certain types of NaV channels (134). A modified ball-and-chain-like model called the hinged lid was proposed, with the lid covering the intracellular mouth of the pore, rather than inserting into it, and attached via two chains on both sides to repeats III and IV (42) (**Figure 1**).

Prokaryotic channels were less helpful as models for investigations of inactivation in $Na^+$ channels, mainly because, much like $K^+$ channels, the prokaryotic $Na^+$ channels form tetramers from four separate subunits and thus lack a linker connecting the individual subunits, where the

inactivation motif in NaV channels is located. Their inactivation is slow and proposed to be of the C type, occurring at the selectivity filter (65, 103).

Cryo-EM structures of eukaryotic NaV channels have led to a revision of the hinged lid model (62, 90, 91, 111). The structures revealed that the IFM motif buries into a hydrophobic niche formed by the pore-lining helices of repeats III and IV, keeping the lid away from the intracellular mouth of the pore. It is still possible to envision a mechanism that would release the IFM motif from the hydrophobic lock to free the lid to cover the intracellular pore mouth; however, an alternative allosteric model for inactivation was proposed in which the IFM motif wedging in between the two pore-lining helices from adjacent repeats would lead to gate closure (91). Further details, structures, and mechanistic studies are needed to elucidate the mechanism.

Exciting new evidence from an NaV channel from coccolithophore *Emiliania huxleyi* (NaVEh), a eukaryotic unicellular phytoplankton living in the ocean, resurrected the classic ball-and-chain inactivation model that had already been shelved for $Na^+$ channels (149). NaVEh is a single-repeat channel similar to the prokaryotic NaV channels (a tetramer composed of four separate subunits, rather than one long polypeptide with four homologous repeats) that does not have the IFM motif. Instead, it has an N terminus with characteristics similar to the inactivation ball of the ball-and-chain mechanism, i.e., a hydrophobic region at the N-terminal tip, and a positively charged region at the base (149). Its cryo-EM structure shows an open activation gate with a helical density inserted about two helical turns up the intracellular gate (149) (**Figure 6*c–d***). The helical density is proposed to inactivate the channel via the ball-and-chain mechanism, since the N-terminus-deleted mutant lacks this density in its cryo-EM structure and loses fast inactivation, and intracellular application of a synthetic N-terminal peptide can partly restore fast inactivation (149). Ball-and-chain N termini are present in NaV channels of other coccolithophores, suggesting that ball-and-chain inactivation is conserved in this taxon and might be essential for tolerating high-$Na^+$ environments (51, 52, 149).

## 6. PHYSIOLOGICAL ROLES FOR BALL-AND-CHAIN INACTIVATION IN $K^+$ CHANNELS

Ion channel inactivation is well-known for shaping the electrical activity of excitable cells; $Na^+$ channel inactivation controls the duration of an action potential by shunting the $Na^+$ influx and allowing the cell membrane to repolarize, and $K^+$ channel inactivation controls the duration and frequency of action potentials and thus the firing rate (54). Below, we discuss a couple of other ways in which ball-and-chain inactivation of $K^+$ channels contributes to a physiological response.

### 6.1. Circadian Clock

The circadian pattern is evolutionarily conserved in human and other organisms, setting daily rhythms in behaviors and physiology (89, 119). In mammals, neurons in the suprachiasmatic nucleus (SCN) of the hypothalamus undergo synchronized daily oscillations to generate diurnal patterns of rhythmic circuits of action potential firing (41, 132). Such circadian rhythms are regulated by BK channels (29, 79, 82). BK-deficient mice still have circadian rhythms, but with smaller day–night variation (29).

Two different BK currents have been described in the SCN, a day and a night current, with different steady-state current magnitudes and inactivation phenotypes (79, 82, 98). The different inactivation phenotypes of the BK currents are mediated by differential day–night expression of the auxiliary β2 subunit, which works by a ball-and-chain mechanism (70, 81, 135). β2-knockout neurons have significantly reduced rhythmicity in BK currents. Similarly, β2-knockout mice have decreased circadian behavioral amplitudes (135).

### 6.2. Ball-and-Chain Inactivation in Sensory Neurons

The sensory system transmits information from peripheral receptors to the central nervous system. Intrinsic and environmental cues, such as hearing, smell, taste, touch, pain, and temperature, are relayed through excitability of sensory neurons (also known as afferent neurons) containing a repertoire of Kv channels (18, 46, 86, 131). The neuronal Kv1.4 channel plays a role in controlling action potential latency and firing frequency (18, 128) and is involved in pain (24, 25, 64, 114, 148). It activates at low voltage and exhibits fast inactivation via the classic ball-and-chain mechanism using an intrinsic N terminus (136). The ball-and-chain inactivation of Kv1.4 can be accelerated upon binding β2, an ancillary subunit with a highly conserved aldo-keto reductase moiety (49, 59, 78, 96, 133). In the presence of β2 substrate and an NADPH cofactor, the Kv1.4-β2 complex slows its inactivation, suggesting the possibility of coupling between intracellular redox states and the excitability of the neuron (49, 133). In addition, Kv1.4 inactivation can be regulated by factors such as $Ca^{2+}$-dependent phosphorylation cascade (107), intracellular hemin (for the Kv1.4-Kvβ complex) (28), and oxidation of the channel (108).

Kv3.4 is a neuronal channel abundant in dorsal root ganglion nociceptors (26, 83) that is essential for axon growth and is also involved in the pain pathway (26, 37, 58, 106, 148). Kv3.4 is activated by high voltage and is fast inactivated through the classic ball-and-chain mechanism by an endogenous N terminus, which contains several protein kinase C (PKC) phosphorylation sites. Phosphorylation of Kv3.4 dramatically slows down inactivation, presumably by altering the structure of the N terminus (5, 105). The phosphatase calcineurin (CaN) seems to play an opposite role to PKC, as inhibition of CaN also decelerates inactivation and slows down repolarization of the action potential (147). In addition, oxidation of the N terminus has also been found to modulate Kv3.4 inactivation (108).

## 7. CONCLUDING REMARKS

In this review, we summarize the discovery of ball-and-chain inactivation and discuss the current understanding of the mechanism. Ball-and-chain inactivation is common in Kv channels and $Ca^{2+}$-gated $K^+$ channels but is limited to unicellular phytoplanktonic NaV channels. The ball-and-chain mechanism shares the conserved feature among channels that fast inactivation involves open pore occlusion by N-terminal inactivation gates. In eukaryotes, ball-and-chain inactivation can be mediated by intermolecular N-terminal balls and modulated by various physiological factors, such as cellular redox states. This highlights the complexity of ball-and-chain inactivation and that regulation of the process is crucial for normal functioning of the cells.

Since the discovery of ball-and-chain inactivation in 1977, only two structures have captured this inactivation, both of which are cryo-EM structures of post-inactivation (open-inactivated) states from two ion channels: MthK and NaVEh. In Kv and BK channels, side windows, which are conserved between the cytosolic T1 domain and the transmembrane domain, have been proposed to be gateways that attract the N-terminal balls due to electrostatic interactions and believed to involve a formation of the pre-inactivation state of the ball-and-chain mechanism. However, there is still no structural verification for the pre-inactivation state, perhaps due to the unstructured nature of the N-terminal balls prior to binding to the channel pore. More structural information, therefore, will enhance our understanding of the ball-and-chain mechanism and enable drug discovery based on the process.

## DISCLOSURE STATEMENT

The authors are not aware of any affiliations, memberships, funding, or financial holdings that might be perceived as affecting the objectivity of this review.

## ACKNOWLEDGMENTS

This work was funded in part by National Institutes of Health grants R01GM088352 and R01GM124451 to C.M.N.

## LITERATURE CITED

1. Ahern CA. 2013. What activates inactivation? *J. Gen. Physiol.* 142:97–100
2. Aldrich RW. 2001. Fifty years of inactivation. *Nature* 411:643–44
3. Aldrich RW, Corey DP, Stevens CF. 1983. A reinterpretation of mammalian sodium channel gating based on single channel recording. *Nature* 306:436–41
4. Aldrich RW, Hoshi T, Zagotta WN. 1990. Differences in gating among amino-terminal variants of Shaker potassium channels. *Cold Spring Harb. Symp. Quant. Biol.* 55:19–27
5. Antz C, Bauer T, Kalbacher H, Frank R, Covarrubias M, et al. 1999. Control of $K^+$ channel gating by protein phosphorylation: structural switches of the inactivation gate. *Nat. Struct. Biol.* 6:146–50
6. Antz C, Fakler B. 1998. Fast inactivation of voltage-gated $K^+$ channels: from cartoon to structure. *News Physiol. Sci.* 13:177–82
7. Antz C, Geyer M, Fakler B, Schott MK, Guy HR, et al. 1997. NMR structure of inactivation gates from mammalian voltage-dependent potassium channels. *Nature* 385:272–75
8. Armstrong CM. 1966. Time course of $TEA^+$-induced anomalous rectification in squid giant axons. *J. Gen. Physiol.* 50:491–503
9. Armstrong CM. 1968. Induced inactivation of the potassium permeability of squid axon membranes. *Nature* 219:1262–63
10. Armstrong CM. 1969. Inactivation of the potassium conductance and related phenomena caused by quaternary ammonium ion injection in squid axons. *J. Gen. Physiol.* 54:553–75
11. Armstrong CM. 1981. Sodium channels and gating currents. *Physiol. Rev.* 61:644–83
12. Armstrong CM, Bezanilla F. 1977. Inactivation of the sodium channel. II. Gating current experiments. *J. Gen. Physiol.* 70:567–90
13. Armstrong CM, Bezanilla F, Rojas E. 1973. Destruction of sodium conductance inactivation in squid axons perfused with pronase. *J. Gen. Physiol.* 62:375–91
14. Bahring R, Vardanyan V, Pongs O. 2004. Differential modulation of Kv1 channel-mediated currents by co-expression of Kvβ3 subunit in a mammalian cell-line. *Mol. Membr. Biol.* 21:19–25
15. Baker K, Salkoff L. 1990. The *Drosophila* Shaker gene codes for a distinctive $K^+$ current in a subset of neurons. *Neuron* 4:129–40
16. Baukrowitz T, Yellen G. 1995. Modulation of $K^+$ current by frequency and external $[K^+]$: a tale of two inactivation mechanisms. *Neuron* 15:951–60
17. Baukrowitz T, Yellen G. 1996. Use-dependent blockers and exit rate of the last ion from the multi-ion pore of a $K^+$ channel. *Science* 271:653–56
18. Benarroch EE. 2015. Ion channels in nociceptors: recent developments. *Neurology* 84:1153–64
19. Bentrop D, Beyermann M, Wissmann R, Fakler B. 2001. NMR structure of the "ball-and-chain" domain of KCNMB2, the β 2-subunit of large conductance $Ca^{2+}$- and voltage-activated potassium channels. *J. Biol. Chem.* 276:42116–21
20. Bett GC, Dinga-Madou I, Zhou Q, Bondarenko VE, Rasmusson RL. 2011. A model of the interaction between N-type and C-type inactivation in Kv1.4 channels. *Biophys. J.* 100:11–21
21. Boiteux C, Posson DJ, TW Allen, Nimigean CM. 2020. Selectivity filter ion binding affinity determines inactivation in a potassium channel. *PNAS* 117:29968–78
22. Catterall WA. 2000. From ionic currents to molecular mechanisms: the structure and function of voltage-gated sodium channels. *Neuron* 26:13–25
23. Catterall WA, Goldin AL, Waxman SG. 2005. International Union of Pharmacology. XLVII. Nomenclature and structure-function relationships of voltage-gated sodium channels. *Pharmacol. Rev.* 57:397–409
24. Chen J, Winston JH, Sarna SK. 2013. Neurological and cellular regulation of visceral hypersensitivity induced by chronic stress and colonic inflammation in rats. *Neuroscience* 248:469–78

25. Chen R, Li YJ, Li JQ, Lv XX, Chen SZ, et al. 2011. Electrical injury alters ion channel expression levels and electrophysiological properties in rabbit dorsal root ganglia neurons. *Burns* 37:304–11
26. Chien LY, Cheng JK, Chu D, Cheng CF, Tsaur ML. 2007. Reduced expression of A-type potassium channels in primary sensory neurons induces mechanical hypersensitivity. *J. Neurosci.* 27:9855–65
27. Choi KL, Aldrich RW, Yellen G. 1991. Tetraethylammonium blockade distinguishes two inactivation mechanisms in voltage-activated $K^+$ channels. *PNAS* 88:5092–95
28. Coburger I, Yang K, Bernert A, Wiesel E, Sahoo N, et al. 2020. Impact of intracellular hemin on N-type inactivation of voltage-gated $K^+$ channels. *Pflugers Arch.* 472:551–60
29. Colwell CS. 2006. BK channels and circadian output. *Nat. Neurosci.* 9:985–86
30. Connor JA, Stevens CF. 1971. Voltage clamp studies of a transient outward membrane current in gastropod neural somata. *J. Physiol.* 213:21–30
31. Cordero-Morales JF, Cuello LG, Perozo E. 2006. Voltage-dependent gating at the KcsA selectivity filter. *Nat. Struct. Mol. Biol.* 13:319–22
32. Cordero-Morales JF, Jogini V, Lewis A, Vasquez V, Cortes DM, et al. 2007. Molecular driving forces determining potassium channel slow inactivation. *Nat. Struct. Mol. Biol.* 14:1062–69
33. Cuello LG, Jogini V, Cortes DM, Perozo E. 2010. Structural mechanism of C-type inactivation in $K^+$ channels. *Nature* 466:203–8
34. Dart C. 2010. Lipid microdomains and the regulation of ion channel function. *J. Physiol.* 588:3169–78
35. Demo SD, Yellen G. 1991. The inactivation gate of the Shaker $K^+$ channel behaves like an open-channel blocker. *Neuron* 7:743–53
36. Dong J, Shi N, Berke I, Chen L, Jiang Y. 2005. Structures of the MthK RCK domain and the effect of $Ca^{2+}$ on gating ring stability. *J. Biol. Chem.* 280:41716–24
37. Duan KZ, Xu Q, Zhang XM, Zhao ZQ, Mei YA, Zhang YQ. 2012. Targeting A-type $K^+$ channels in primary sensory neurons for bone cancer pain in a rat model. *Pain* 153:562–74
38. Fan C, Sukomon N, Flood E, Rheinberger J, Allen TW, Nimigean CM. 2020. Ball-and-chain inactivation in a calcium-gated potassium channel. *Nature* 580:288–93
39. Foster CD, Chung S, Zagotta WN, Aldrich RW, Levitan IB. 1992. A peptide derived from the *shaker* B $K^+$ channel produces short and long blocks of reconstituted $Ca^{2+}$-dependent $K^+$ channels. *Neuron* 9:229–36
40. Geiger JR, Jonas P. 2000. Dynamic control of presynaptic $Ca^{2+}$ inflow by fast-inactivating $K^+$ channels in hippocampal mossy fiber boutons. *Neuron* 28:927–39
41. Gillette MU, Tischkau SA. 1999. Suprachiasmatic nucleus: the brain's circadian clock. *Recent Prog. Horm. Res.* 54:33–58; discussion 58–59
42. Goldin AL. 2003. Mechanisms of sodium channel inactivation. *Curr. Opin. Neurobiol.* 13:284–90
43. Gonzalez-Perez V, Lingle CJ. 2019. Regulation of BK channels by β and γ subunits. *Annu. Rev. Physiol.* 81:113–37
44. Gonzalez-Perez V, Zeng XH, Henzler-Wildman K, Lingle CJ. 2012. Stereospecific binding of a disordered peptide segment mediates BK channel inactivation. *Nature* 485:133–36
45. Gulbis JM, Zhou M, Mann S, MacKinnon R. 2000. Structure of the cytoplasmic β subunit-T1 assembly of voltage-dependent $K^+$ channels. *Science* 289:123–27
46. Haberberger RV, Barry C, Dominguez N, Matusica D. 2019. Human dorsal root ganglia. *Front Cell Neurosci* 13:271
47. Heginbotham L, Abramson T, MacKinnon R. 1992. A functional connection between the pores of distantly related ion channels as revealed by mutant $K^+$ channels. *Science* 258:1152–55
48. Heginbotham L, Lu Z, Abramson T, MacKinnon R. 1994. Mutations in the $K^+$ channel signature sequence. *Biophys. J.* 66:1061–67
49. Heinemann SH, Hoshi T. 2006. Multifunctional potassium channels: electrical switches and redox enzymes, all in one. *Sci. STKE* 2006:pe33
50. Heinemann SH, Rettig J, Wunder F, Pongs O. 1995. Molecular and functional characterization of a rat brain $K_v\beta 3$ potassium channel subunit. *FEBS Lett.* 377:383–89
51. Helliwell KE, Chrachri A, Koester JA, Wharam S, Taylor AR, et al. 2020. A novel single-domain $Na^+$-selective voltage-gated channel in photosynthetic eukaryotes. *Plant Physiol.* 184:1674–83

52. Helliwell KE, Chrachri A, Koester JA, Wharam S, Verret F, et al. 2019. Alternative mechanisms for fast $Na^+/Ca^{2+}$ signaling in eukaryotes via a novel class of single-domain voltage-gated channels. *Curr. Biol.* 29:1503–11.e6
53. Hille B. 1978. Ionic channels in excitable membranes. Current problems and biophysical approaches. *Biophys. J.* 22:283–94
54. Hille B. 2001. *Ion Channels of Excitable Membranes*. Sunderland, MA: Sinauer Assoc.
55. Hodgkin AL, Huxley AF. 1952. A quantitative description of membrane current and its application to conduction and excitation in nerve. *J. Physiol.* 117:500–44
56. Hoshi T, Zagotta WN, Aldrich RW. 1990. Biophysical and molecular mechanisms of Shaker potassium channel inactivation. *Science* 250:533–38
57. Hoshi T, Zagotta WN, Aldrich RW. 1991. Two types of inactivation in Shaker $K^+$ channels: effects of alterations in the carboxy-terminal region. *Neuron* 7:547–56
58. Huang CY, Lien CC, Cheng CF, Yen TY, Chen CJ, Tsaur ML. 2017. $K^+$ channel Kv3.4 is essential for axon growth by limiting the influx of $Ca^{2+}$ into growth cones. *J. Neurosci.* 37:4433–49
59. Hyndman D, Bauman DR, Heredia VV, Penning TM. 2003. The aldo-keto reductase superfamily homepage. *Chem. Biol. Interact.* 143–44:621–31
60. Isacoff EY, Jan YN, Jan LY. 1991. Putative receptor for the cytoplasmic inactivation gate in the Shaker $K^+$ channel. *Nature* 353:86–90
61. Jan LY, Jan YN. 1992. Structural elements involved in specific $K^+$ channel functions. *Annu. Rev. Physiol.* 54:537–55
62. Jiang D, Shi H, Tonggu L, Gamal El-Din TM, Lenaeus MJ, et al. 2020. Structure of the cardiac sodium channel. *Cell* 180:122–34.e10
63. Jiang Y, Lee A, Chen J, Cadene M, Chait BT, MacKinnon R. 2002. Crystal structure and mechanism of a calcium-gated potassium channel. *Nature* 417:515–22
64. Kim DS, Choi JO, Rim HD, Cho HJ. 2002. Downregulation of voltage-gated potassium channel α gene expression in dorsal root ganglia following chronic constriction injury of the rat sciatic nerve. *Brain Res. Mol. Brain Res.* 105:146–52
65. Koishi R, Xu H, Ren D, Navarro B, Spiller BW, et al. 2004. A superfamily of voltage-gated sodium channels in bacteria. *J. Biol. Chem.* 279:9532–38
66. Kramer RH, Goulding E, Siegelbaum SA. 1994. Potassium channel inactivation peptide blocks cyclic nucleotide-gated channels by binding to the conserved pore domain. *Neuron* 12:655–62
67. Kreusch A, Pfaffinger PJ, Stevens CF, Choe S. 1998. Crystal structure of the tetramerization domain of the Shaker potassium channel. *Nature* 392:945–48
68. Kuo MM, Maslennikov I, Molden B, Choe S. 2008. The desensitization gating of the MthK $K^+$ channel is governed by its cytoplasmic amino terminus. *PLOS Biol.* 6:e223
69. Kurata HT, Fedida D. 2006. A structural interpretation of voltage-gated potassium channel inactivation. *Prog. Biophys. Mol. Biol.* 92:185–208
70. Li Q, Yan J. 2016. Modulation of BK channel function by auxiliary β and γ subunits. *Int. Rev. Neurobiol.* 128:51–90
71. Li Y, Berke I, Chen L, Jiang Y. 2007. Gating and inward rectifying properties of the MthK $K^+$ channel with and without the gating ring. *J. Gen. Physiol.* 129:109–20
72. Lingle CJ, Zeng XH, Ding JP, Xia XM. 2001. Inactivation of BK channels mediated by the $NH_2$ terminus of the β3b auxiliary subunit involves a two-step mechanism: possible separation of binding and blockade. *J. Gen. Physiol.* 117:583–605
73. Lo MV, Shrager P. 1981. Block and inactivation of sodium channels in nerve by amino acid derivatives. II. Dependence on temperature and drug concentration. *Biophys. J.* 35:45–57
74. Long SB, Campbell EB, MacKinnon R. 2005. Crystal structure of a mammalian voltage-dependent Shaker family $K^+$ channel. *Science* 309:897–903
75. Lopez-Barneo J, Hoshi T, Heinemann SH, Aldrich RW. 1993. Effects of external cations and mutations in the pore region on C-type inactivation of Shaker potassium channels. *Recept. Channels* 1(1):61–71
76. MacKinnon R, Aldrich RW, Lee AW. 1993. Functional stoichiometry of Shaker potassium channel inactivation. *Science* 262:757–59

77. Matulef K, Annen AW, Nix JC, Valiyaveetil FI. 2016. Individual ion binding sites in the $K^+$ channel play distinct roles in C-type inactivation and in recovery from inactivation. *Structure* 24:750–61
78. McCormack T, McCormack K. 1994. Shaker $K^+$ channel β subunits belong to an NAD(P)H-dependent oxidoreductase superfamily. *Cell* 79:1133–35
79. Meredith AL, Wiler SW, Miller BH, Takahashi JS, Fodor AA, et al. 2006. BK calcium-activated potassium channels regulate circadian behavioral rhythms and pacemaker output. *Nat. Neurosci.* 9:1041–49
80. Molina ML, Barrera FN, Encinar JA, Renart ML, Fernandez AM, et al. 2008. N-type inactivation of the potassium channel KcsA by the Shaker B "ball" peptide: mapping the inactivating peptide-binding epitope. *J. Biol. Chem.* 283:18076–85
81. Montgomery JR, Meredith AL. 2012. Genetic activation of BK currents in vivo generates bidirectional effects on neuronal excitability. *PNAS* 109:18997–9002
82. Montgomery JR, Whitt JP, Wright BN, Lai MH, Meredith AL. 2013. Mis-expression of the BK $K^+$ channel disrupts suprachiasmatic nucleus circuit rhythmicity and alters clock-controlled behavior. *Am. J. Physiol. Cell Physiol.* 304: C299–311
83. Muqeem T, Ghosh B, Pinto V, Lepore AC, Covarrubias M. 2018. Regulation of nociceptive glutamatergic signaling by presynaptic Kv3.4 channels in the rat spinal dorsal horn. *J. Neurosci.* 38:3729–40
84. Murrell-Lagnado RD, Aldrich RW. 1993. Interactions of amino terminal domains of Shaker K channels with a pore blocking site studied with synthetic peptides. *J. Gen. Physiol.* 102:949–75
85. Nakajima S. 1966. Analysis of K inactivation and TEA action in the supramedullary cells of puffer. *J. Gen. Physiol.* 49:629–40
86. Nascimento AI, Mar FM, Sousa MM. 2018. The intriguing nature of dorsal root ganglion neurons: linking structure with polarity and function. *Prog. Neurobiol.* 168:86–103
87. Nonner W. 1980. Relations between the inactivation of sodium channels and the immobilization of gating charge in frog myelinated nerve. *J. Physiol.* 299:573–603
88. Oliver D, Lien CC, Soom M, Baukrowitz T, Jonas P, Fakler B. 2004. Functional conversion between A-type and delayed rectifier $K^+$ channels by membrane lipids. *Science* 304:265–70
89. Palm D, Uzoni A, Simon F, Fischer M, Coogan A, et al. 2021. Evolutionary conservations, changes of circadian rhythms and their effect on circadian disturbances and therapeutic approaches. *Neurosci. Biobehav. Rev.* 128:21–34
90. Pan X, Li Z, Huang X, Huang G, Gao S, et al. 2019. Molecular basis for pore blockade of human $Na^+$ channel $Na_v1.2$ by the μ-conotoxin KIIIA. *Science* 363:1309–13
91. Pan X, Li Z, Zhou Q, Shen H, Wu K, et al. 2018. Structure of the human voltage-gated sodium channel Nav1.4 in complex with β1. *Science* 362:eaau2486
92. Papazian DM, Schwarz TL, Tempel BL, Jan YN, Jan LY. 1987. Cloning of genomic and complementary DNA from Shaker, a putative potassium channel gene from *Drosophila*. *Science* 237:749–53
93. Patton DE, West JW, Catterall WA, Goldin AL. 1992. Amino acid residues required for fast $Na^+$-channel inactivation: charge neutralizations and deletions in the III-IV linker. *PNAS* 89:10905–9
94. Pau V, Zhou Y, Ramu Y, Xu Y, Lu Z. 2017. Crystal structure of an inactivated mutant mammalian voltage-gated $K^+$ channel. *Nat. Struct. Mol. Biol.* 24:857–65
95. Pau VP, Abarca-Heidemann K, Rothberg BS. 2010. Allosteric mechanism of $Ca^{2+}$ activation and $H^+$-inhibited gating of the MthK $K^+$ channel. *J. Gen. Physiol.* 135:509–26
96. Peri R, Wible BA, Brown AM. 2001. Mutations in the Kvβ2 binding site for NADPH and their effects on Kv1.4. *J. Biol. Chem.* 276:738–41
97. Pfaffinger PJ. 2013. A conserved pre-block interaction motif regulates potassium channel activation and N-type inactivation. *PLOS ONE* 8:e79891
98. Pitts GR, Ohta H, McMahon DG. 2006. Daily rhythmicity of large-conductance $Ca^{2+}$-activated $K^+$ currents in suprachiasmatic nucleus neurons. *Brain Res.* 1071:54–62
99. Pongs O, Schwarz JR. 2010. Ancillary subunits associated with voltage-dependent $K^+$ channels. *Physiol. Rev.* 90:755–96
100. Posson DJ, Rusinova R, Andersen OS, Nimigean CM. 2015. Calcium ions open a selectivity filter gate during activation of the MthK potassium channel. *Nat. Commun.* 6:8342

101. Prince-Carter A, Pfaffinger PJ. 2009. Multiple intermediate states precede pore block during N-type inactivation of a voltage-gated potassium channel. *J. Gen. Physiol.* 134:15–34
102. Rasmusson RL, Morales MJ, Wang S, Liu S, Campbell DL, et al. 1998. Inactivation of voltage-gated cardiac $K^+$ channels. *Circ. Res.* 82:739–50
103. Ren D, Navarro B, Xu H, Yue L, Shi Q, Clapham DE. 2001. A prokaryotic voltage-gated sodium channel. *Science* 294:2372–75
104. Rettig J, Heinemann SH, Wunder F, Lorra C, Parcej DN, et al. 1994. Inactivation properties of voltage-gated $K^+$ channels altered by presence of β-subunit. *Nature* 369:289–94
105. Ritter DM, Ho C, O'Leary ME, Covarrubias M. 2012. Modulation of Kv3.4 channel N-type inactivation by protein kinase C shapes the action potential in dorsal root ganglion neurons. *J. Physiol.* 590:145–61
106. Ritter DM, Zemel BM, Lepore AC, Covarrubias M. 2015. Kv3.4 channel function and dysfunction in nociceptors. *Channels* 9:209–17
107. Roeper J, Lorra C, Pongs O. 1997. Frequency-dependent inactivation of mammalian A-type $K^+$ channel KV1.4 regulated by $Ca^{2+}$/calmodulin-dependent protein kinase. *J. Neurosci.* 17:3379–91
108. Ruppersberg JP, Stocker M, Pongs O, Heinemann SH, Frank R, Koenen M. 1991. Regulation of fast inactivation of cloned mammalian $I_K$(A) channels by cysteine oxidation. *Nature* 352:711–14
109. Schott MK, Antz C, Frank R, Ruppersberg JP, Kalbitzer HR. 1998. Structure of the inactivating gate from the Shaker voltage gated $K^+$ channel analyzed by NMR spectroscopy. *Eur. Biophys. J.* 27:99–104
110. Schwarz TL, Tempel BL, Papazian DM, Jan YN, Jan LY. 1988. Multiple potassium-channel components are produced by alternative splicing at the Shaker locus in *Drosophila*. *Nature* 331:137–42
111. Shen H, Liu D, Wu K, Lei J, Yan N. 2019. Structures of human Nav1.7 channel in complex with auxiliary subunits and animal toxins. *Science* 363:1303–8
112. Sokolova O, Kolmakova-Partensky L, Grigorieff N. 2001. Three-dimensional structure of a voltage-gated potassium channel at 2.5 nm resolution. *Structure* 9:215–20
113. Stuhmer W, Conti F, Suzuki H, Wang XD, Noda M, et al. 1989. Structural parts involved in activation and inactivation of the sodium channel. *Nature* 339:597–603
114. Takeda M, Tanimoto T, Nasu M, Matsumoto S. 2008. Temporomandibular joint inflammation decreases the voltage-gated $K^+$ channel subtype 1.4-immunoreactivity of trigeminal ganglion neurons in rats. *Eur. J. Pain* 12:189–95
115. Tan XF, Bae C, Stix R, Fernandez-Marino AI, Huffer K, et al. 2022. Structure of the Shaker Kv channel and mechanism of slow C-type inactivation. *Sci. Adv.* 8:eabm7814
116. Tanouye MA, Kamb CA, Iverson LE, Salkoff L. 1986. Genetics and molecular biology of ionic channels in *Drosophila*. *Annu. Rev. Neurosci.* 9:255–76
117. Tao X, Hite RK, MacKinnon R. 2017. Cryo-EM structure of the open high-conductance $Ca^{2+}$-activated $K^+$ channel. *Nature* 541:46–51
118. Tao X, MacKinnon R. 2019. Molecular structures of the human Slo1 $K^+$ channel in complex with β4. *eLife* 8:e51409
119. Tarrant AM, Reitzel AM. 2013. Introduction to the symposium—keeping time during evolution: conservation and innovation of the circadian clock. *Integr. Comp. Biol.* 53:89–92
120. Tempel BL, Papazian DM, Schwarz TL, Jan YN, Jan LY. 1987. Sequence of a probable potassium channel component encoded at Shaker locus of *Drosophila*. *Science* 237:770–75
121. Timpe LC, Jan YN, Jan LY. 1988. Four cDNA clones from the Shaker locus of *Drosophila* induce kinetically distinct A-type potassium currents in *Xenopus* oocytes. *Neuron* 1:659–67
122. Timpe LC, Schwarz TL, Tempel BL, Papazian DM, Jan YN, Jan LY. 1988. Expression of functional potassium channels from Shaker cDNA in *Xenopus* oocytes. *Nature* 331:143–45
123. Toro L, Stefani E, Latorre R. 1992. Internal blockade of a $Ca^{2+}$-activated $K^+$ channel by Shaker B inactivating "ball" peptide. *Neuron* 9:237–45
124. Uebele VN, Lagrutta A, Wade T, Figueroa DJ, Liu Y, et al. 2000. Cloning and functional expression of two families of β-subunits of the large conductance calcium-activated $K^+$ channel. *J. Biol. Chem.* 275:23211–18
125. Valiyaveetil FI. 2017. A glimpse into the C-type-inactivated state for a potassium channel. *Nat. Struct. Mol. Biol.* 24:787–88

126. Vassilev P, Scheuer T, Catterall WA. 1989. Inhibition of inactivation of single sodium channels by a site-directed antibody. *PNAS* 86:8147–51
127. Vassilev PM, Scheuer T, Catterall WA. 1988. Identification of an intracellular peptide segment involved in sodium channel inactivation. *Science* 241:1658–61
128. Vydyanathan A, Wu ZZ, Chen SR, Pan HL. 2005. A-type voltage-gated $K^+$ currents influence firing properties of isolectin B4-positive but not isolectin B4-negative primary sensory neurons. *J. Neurophysiol.* 93:3401–9
129. Wallner M, Meera P, Toro L. 1999. Molecular basis of fast inactivation in voltage and $Ca^{2+}$-activated $K^+$ channels: a transmembrane β-subunit homolog. *PNAS* 96:4137–42
130. Wang YW, Ding JP, Xia XM, Lingle CJ. 2002. Consequences of the stoichiometry of Slo1 α and auxiliary β subunits on functional properties of large-conductance $Ca^{2+}$-activated $K^+$ channels. *J. Neurosci.* 22:1550–61
131. Waxman SG, Zamponi GW. 2014. Regulating excitability of peripheral afferents: emerging ion channel targets. *Nat. Neurosci.* 17:153–63
132. Welsh DK, Takahashi JS, Kay SA. 2010. Suprachiasmatic nucleus: cell autonomy and network properties. *Annu. Rev. Physiol.* 72:551–77
133. Weng J, Cao Y, Moss N, Zhou M. 2006. Modulation of voltage-dependent Shaker family potassium channels by an aldo-keto reductase. *J. Biol. Chem.* 281:15194–200
134. West JW, Patton DE, Scheuer T, Wang Y, Goldin AL, Catterall WA. 1992. A cluster of hydrophobic amino acid residues required for fast $Na^+$-channel inactivation. *PNAS* 89:10910–14
135. Whitt JP, Montgomery JR, Meredith AL. 2016. BK channel inactivation gates daytime excitability in the circadian clock. *Nat. Commun.* 7:10837
136. Wissmann R, Bildl W, Oliver D, Beyermann M, Kalbitzer HR, et al. 2003. Solution structure and function of the "tandem inactivation domain" of the neuronal A-type potassium channel Kv1.4. *J. Biol. Chem.* 278:16142–50
137. Xia XM, Ding JP, Lingle CJ. 2003. Inactivation of BK channels by the NH2 terminus of the β2 auxiliary subunit: an essential role of a terminal peptide segment of three hydrophobic residues. *J. Gen. Physiol.* 121:125–48
138. Xu Y, McDermott AE. 2019. Inactivation in the potassium channel KcsA. *J. Struct. Biol. X* 3:100009
139. Yan J, Li Q, Aldrich RW. 2016. Closed state-coupled C-type inactivation in BK channels. *PNAS* 113:6991–96
140. Yang H, Zhang G, Cui J. 2015. BK channels: multiple sensors, one activation gate. *Front. Physiol.* 6:29
141. Ye S, Li Y, Chen L, Jiang Y. 2006. Crystal structures of a ligand-free MthK gating ring: insights into the ligand gating mechanism of $K^+$ channels. *Cell* 126:1161–73
142. Yeh JZ, Narahashi T. 1977. Kinetic analysis of pancuronium interaction with sodium channels in squid axon membranes. *J. Gen. Physiol.* 69:293–323
143. Yellen G. 1998. The moving parts of voltage-gated ion channels. *Q. Rev. Biophys.* 31:239–95
144. Zadek B, Nimigean CM. 2006. Calcium-dependent gating of MthK, a prokaryotic potassium channel. *J. Gen. Physiol.* 127:673–85
145. Zagotta WN, Hoshi T, Aldrich RW. 1989. Gating of single Shaker potassium channels in *Drosophila* muscle and in *Xenopus* oocytes injected with Shaker mRNA. *PNAS* 86:7243–47
146. Zagotta WN, Hoshi T, Aldrich RW. 1990. Restoration of inactivation in mutants of Shaker potassium channels by a peptide derived from ShB. *Science* 250:568–71
147. Zemel BM, Muqeem T, Brown EV, Goulao M, Urban MW, et al. 2017. Calcineurin dysregulation underlies spinal cord injury-induced $K^+$ channel dysfunction in DRG neurons. *J. Neurosci.* 37:8256–72
148. Zemel BM, Ritter DM, Covarrubias M, Muqeem T. 2018. A-type KV channels in dorsal root ganglion neurons: diversity, function, and dysfunction. *Front. Mol. Neurosci.* 11:253
149. Zhang J, Shi Y, Fan J, Chen H, Xia Z, et al. 2022. N-type fast inactivation of a eukaryotic voltage-gated sodium channel. *Nat. Commun.* 13:2713
150. Zhou M, Morais-Cabral JH, Mann S, MacKinnon R. 2001. Potassium channel receptor site for the inactivation gate and quaternary amine inhibitors. *Nature* 411:657–61
151. Zhou Y, Morais-Cabral JH, Kaufman A, MacKinnon R. 2001. Chemistry of ion coordination and hydration revealed by a $K^+$ channel-Fab complex at 2.0 Å resolution. *Nature* 414:43–48